

# Characterization and Modeling of Bias Dependent Breakdown and Self-Heating in GaInP/GaAs Power HBT to Improve High Power Amplifier Design

Sylvain Heckmann, Raphaël Sommet, Jean-Michel Nébus, Jean-Claude Jacquet, Didier Floriot, Philippe Auxemery, and Raymond Quéré, *Senior Member, IEEE*

**Abstract**—It is usual to say that power GaInP/GaAs heterojunction bipolar transistors (HBTs) have got a lot of advantages for power amplification at microwave frequencies, because of their high gain and high power density. Furthermore, the possibility to control the base biasing conditions (voltage, current, self-bias control) compared to a field-effect transistor offers additive degrees of freedom to make a tradeoff between linearity and power-added efficiency. Nevertheless existing devices are limited because of the relatively low breakdown voltage whereas high collector voltage swings are required to achieve high power. This drawback makes them not appropriate to be used in the next generation of mobile communication base station or radar systems. Silicon technologies such as LDMOS and III–V devices (MESFET and HFET) [1], present competitive performances in term of high power level but for medium power added efficiency. Important improvements have been done in the last years which make possible large breakdown voltages on GaInP/GaAs HBTs. Breakdown value close to 67 V has been achieved. The aim of this work is to significantly improve the modeling of the breakdown voltage on that kind of transistor. Furthermore the in depth characterization and modeling of self-heating effects has been greatly improved in order to improve thermal management solutions which enable to enhanced design solutions of HBT high power amplifiers.

**Index Terms**—Breakdown modeling, heterojunction bipolar transistors (HBTs), pulsed measurement, thermal characterization.

## I. INTRODUCTION

AS HAS BEEN demonstrated in the past, the power heterojunction bipolar transistor (HBT) technology offers many ways to address all the needs in term of power, efficiency high reliability for applications ranging from *L*- to *Ku*-bands [2]. In *L*-band, high power are needed to address next generation of base station for mobile communications. Increasing power could be done following two methods: by the operating voltage or the operating current. The first way has been chosen because having high voltage offers the advantage to provide high

Manuscript received April 6, 2002; revised August 23, 2002. This work was supported by the Thales Air Defense Business Group and by the French MoD under Contract 00-34-063.

S. Heckmann, R. Sommet, J.-M. Nébus, and R. Quéré are with the Faculté des Sciences, Institut de Recherche en Communications Optiques et Microondes, Unité Mixte de Recherche, 87060 Limoges Cedex, France (e-mail: sylvain.heckmann@ircm.unilim.fr).

J.-C. Jacquet and D. Floriot are with the Thales Research and Technology Laboratory France, 91404 Orsay Cedex, France.

P. Auxemery is with United Monolithic Semiconductors, 91404 Orsay Cedex, France.

Digital Object Identifier 10.1109/TMTT.2002.805191

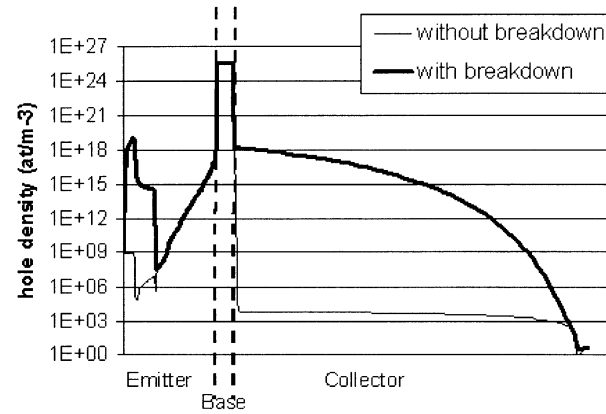


Fig. 1. Hole density along structure calculated by 1-D physical simulation in two cases: impact ionizations are take into account (thick line) or are not take into account (thin line).

power amplifiers with benefit of large output voltage swings. Furthermore, high load impedances make easier the design of output matching circuits. For base station applications, the breakdown value of GaInP/GaAs HBTs has been strongly increased, keeping constant RF performances [3]. To achieve this result, the collector thickness and the collector doping have been optimized to obtain the best tradeoff between high breakdown and high current standing values. Thus, in comparison with previous published results or manufactured devices, the maximum operating collector voltage is increased by a factor three. Such devices will be able to address third-generation cellular base station where LDMOS and Si bipolar junction transistors (Si-BJTs) are dominant. Due to their high power density, HBTs will be also great candidates for modern *S*- and *X*-bands and radar applications. For operating at high collector voltage, circuit designers need to know accurately the limitations due to breakdown and the prejudicial aspect due to self-heating effects. Several papers have been published on this topic based on physical modeling approach [4], [5]. In this paper, we present an improved nonlinear circuit based model compatible with commercial computer-aided design (CAD) packages and validated by measurements.

## II. BREAKDOWN MEASUREMENT AND MODELING

### A. Breakdown Description

At high collector operating voltage, impact ionizations due to high electric field create electron–hole pairs in the depleted

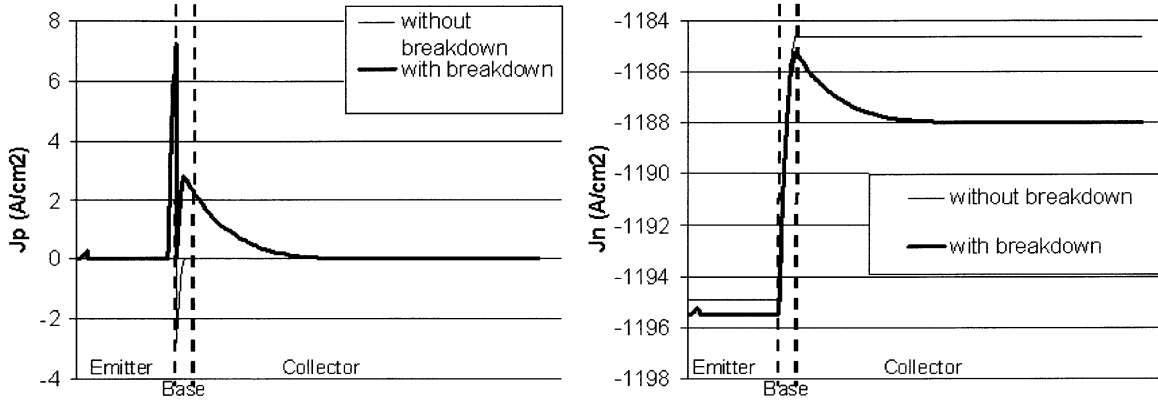


Fig. 2. Electron and hole current density calculated by 1-D physical simulation in two cases: impact ionizations are taken into account (thick line) or are not taken into account (thin line).

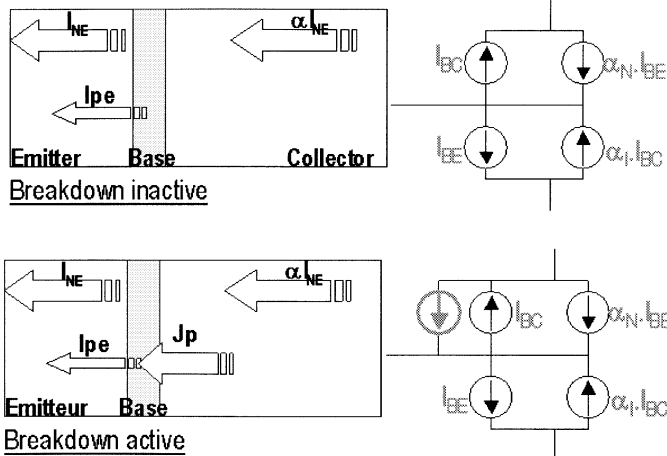


Fig. 3. Representation of the current direction on the transistor structure, impact on electrical model.

collector region that induce high peak electric field. It is the reason why the avalanche current is located in the base-collector (BC) depletion region [6].

Holes coming from electron-hole pairs created during impact-ionization drift toward base because of the high electric field and contribute to the decreasing of the base current by recombining with the electrons coming from the emitter. The value for which the base current becomes negative is related to the definition of  $BV_{CE0}$  ( $I_B = 0$ ).

If the external base biasing current is forced by a (high impedance) current source, the continuous (dc) part of the BC breakdown current feeds back the base-emitter junction. Therefore the base-emitter voltage increases. For one hole coming from collector region,  $b$  electrons are injected into the collector by contributing to a cumulative effect. More electrons are injected from the base to the collector creating more hole-electron pairs. An irreversible breakdown occurs until the device failure (cumulative effect). Figs. 1 and 2 which show one-dimensional (1-D) physical simulation [7] illustrate this mechanism. The simulator we used is a 1-D drift diffusion simulator. That kind of simulator is accurate enough because of high thickness collector structure we use [8].

An electrical representation of that phenomenon is reported in Fig. 3 with an additional current source between base and

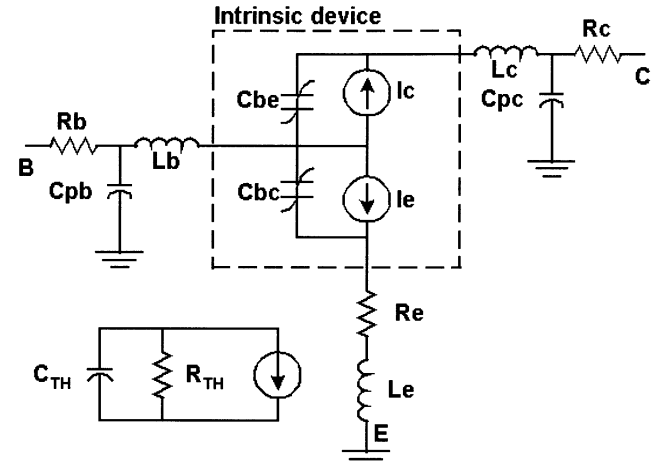


Fig. 4. Large-signal HBT model including self-heating.

collector. Note that this current source could be included in the existing source by the way of a modification of the current gain such as it will be seen in the next part.

In the case of an external base-emitter biasing voltage source (low impedance), the dc part of the BC breakdown current is shunted by the external base biasing circuit (no more cumulative effect). A negative base current is observed and an irreversible BC breakdown occurs at a higher dynamic collector voltage compared to the previous case (constant dc base current control).

This phenomenon, commonly known as  $BV_{CEopen}$  and  $BV_{CEshort}$  in bipolar transistors has been reported as static (dc) breakdown conditions. It makes sense to use common base topology for power amplification.

In comparison with the common base topology, the common emitter topology presents the advantage to exhibit higher input impedance making easier the design of input matching circuit that is a critical step for HBT power amplification design.

In this paper, we point out that the static common emitter breakdown voltage is too much conservative. Under dynamic (RF) operation mode, the collector voltage swing can go beyond the static limitation without damaging the transistor.

Furthermore, as far as the dc base biasing conditions are carefully controlled, a common-emitter configuration of HBT can be

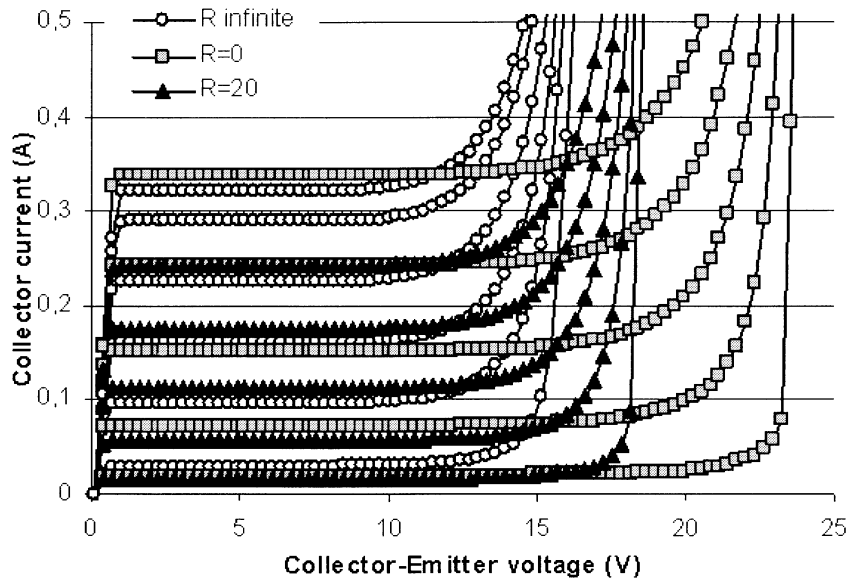


Fig. 5. Isothermal  $I$ - $V$  characteristics simulated in three cases: constant base bias voltage (■:  $R = 0$ ), constant dc base voltage supply with 20-W series base resistor (▲:  $R = 20$  W self-bias condition) and last with constant base current (circle).

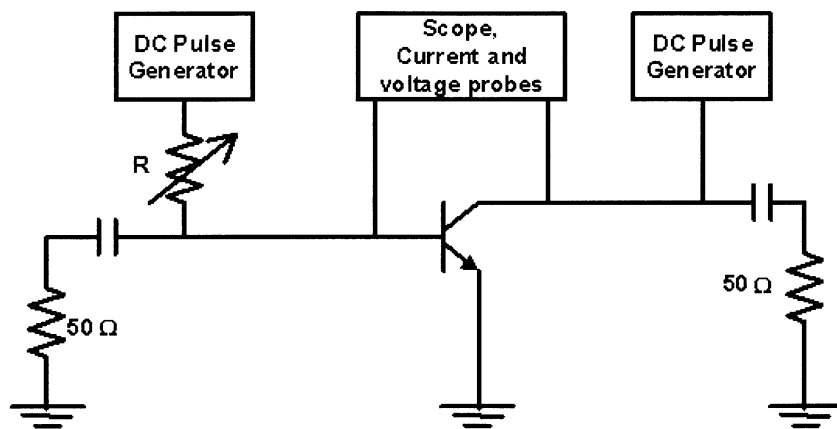


Fig. 6. Pulse measurement set up:  $R$  monitors equivalent impedance of the base supply.

used for very large power amplification at microwave frequencies.

#### B. Breakdown Modeling

Physical simulations validate T-shape configuration as electrical model. The electrical topology is derived from the Ebers-Moll equations. Such a configuration leads to clearly identify the origin of each current in the transistor.

The current sources  $I_C$  and  $I_E$  include the leakage current part and the self-heating (see Fig. 4). The equations of the different nonlinear capacitors have already been published [9].

Here we explain how the model has been modified to include the breakdown behavior by the way of the inconstant  $\alpha_F^*$  term

$$I_C = I_{SC}(T_j) \cdot \left( \exp^{(q \cdot V_{bc})/(Nc \cdot k \cdot T_j)} - 1 \right) - I_{SE}(T_j) \cdot \left( \exp^{(q \cdot V_{be})/(Ne \cdot k \cdot T_j)} - 1 \right) \cdot \alpha_F^* + I_{SFC}(T_j) \cdot \left( \exp^{(q \cdot V_{bc})/(Nfc \cdot k \cdot T_j)} - 1 \right). \quad (1)$$

The dominant part of this current is the term depending on  $V_{BE}$

$$I_E = I_{SE}(T_j) \cdot \left( \exp^{(q \cdot V_{be})/(Ne \cdot k \cdot T_j)} - 1 \right) - I_{SC}(T_j) \cdot \left( \exp^{(q \cdot V_{bc})/(Nc \cdot k \cdot T_j)} - 1 \right) \cdot \alpha_R + I_{SFE}(T_j) \cdot \left( \exp^{(q \cdot V_{be})/(Nfe \cdot k \cdot T_j)} - 1 \right) \quad (2)$$

where the common base current gain is defined by the following equation [10]:

$$\alpha_F^* = \alpha_F \cdot M \quad (3)$$

and the multiplication factor by

$$M = \frac{1}{1 - \left( \frac{V_{CB}}{BV_{CBO}} \right)^n}. \quad (4)$$

With this approach the breakdown limit depends on the base biasing conditions (see Fig. 5).

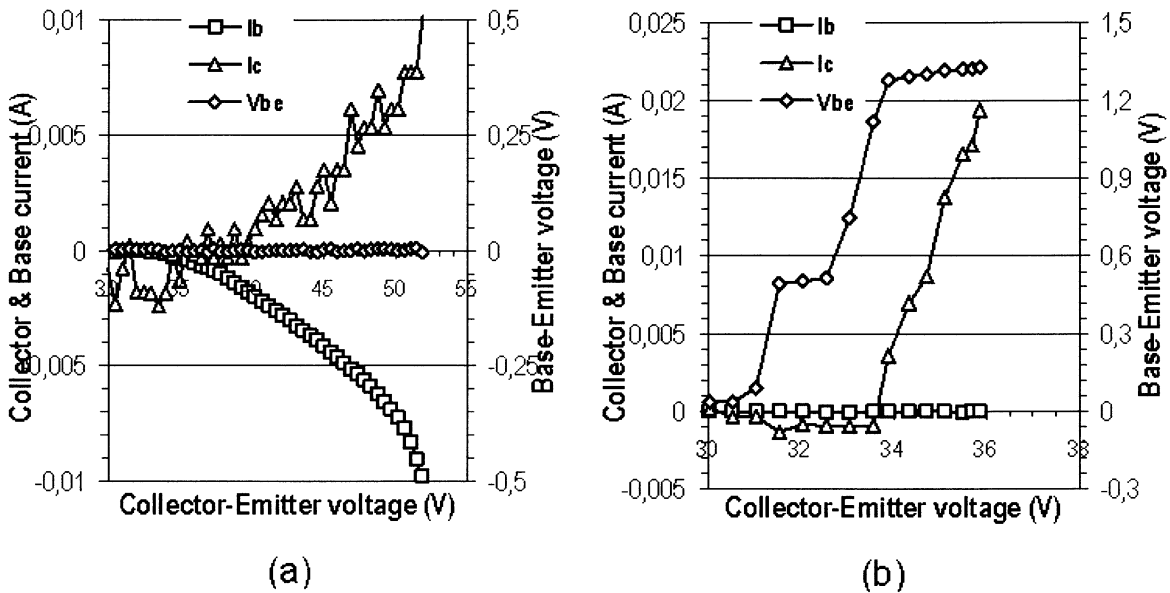


Fig. 7. Breakdown measurement. (a) Monitoring at constant base voltage. (b) Monitoring at constant base current.

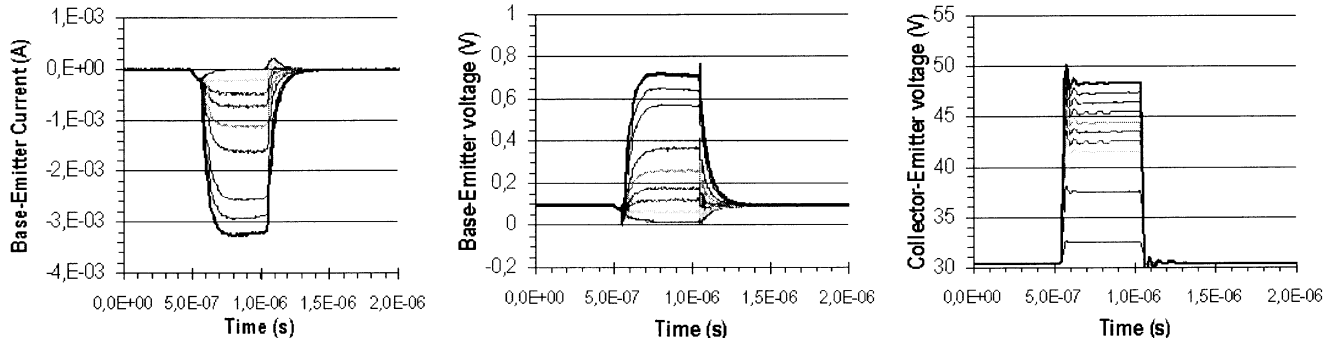


Fig. 8. Time-domain pulse waveform during breakdown measurement when base-emitter voltage is set to 0 V for different collector emitter pulse level.

Because of the influence of the multiplication factor ( $M$ ) on the common base current gain ( $\alpha_F$ ), it is possible to differentiate common base and common emitter breakdown voltages.

A well-known relation is used to link the common base  $BV_{CB0}$  and the common emitter  $BV_{CE0}$  breakdown voltages

$$BV_{CE0} = BV_{CB0} \cdot (1 - \alpha_F)^n. \quad (5)$$

### C. Static Breakdown Measurements

In order to characterize and model the breakdown effect in GaInP/GaAs HBTs, we have performed quasi-isothermal pulsed  $I$ - $V$  measurements on our pulsed measurement setup [11]. Pulsewidth and recurrence were set, respectively, to 500 ns and 6 ms. A schematic of the test bench is given in Fig. 6. A 16 fingers of  $2 \times 70 \mu\text{m}^2$  HBT with 3- $\mu\text{m}$ -thick collector was used to validate the test configurations.

In the  $I_C$  ( $V_{CE}$ ) plan, we scanned the collector-base (CB) breakdown area for two different conditions.

Case 1) Keeping constant the base-emitter voltage at 0 V, we measured the pulsed collector current versus the pulsed collector-emitter voltage.

Case 2) The same measurements have been performed keeping constant a very low base current.

The results are focused on breakdown area and depicted in Fig. 7(a) and (b).

In case 1), the breakdown occurs for a collector emitter voltage of 55 V. Note that the base current has a negative value. It is thus experimentally demonstrated that the breakdown current generated in the base-collector junction can be collected in the base biasing circuit, if the impedance presented at the base bias port is small enough in comparison with the impedance presented by the base-emitter junction. Therefore the base-emitter voltage does not increase and the maximum value of the collector-emitter voltage for which an irreversible breakdown occurs is much higher.

In case 2), current source close to 0 mA, the breakdown occurs at 34 V of collector emitter voltage.

Fig. 8 shows time-domain pulse waveforms in the case of an external constant base-emitter voltage (set to 0 V in this case).

### D. Load-Pull Measurements

Load-pull measurements were performed at 2 GHz on a second set of transistors with a collector layer thickness close to 1  $\mu\text{m}$ . For this last value, the devices have 16 V of  $BV_{CE0}$

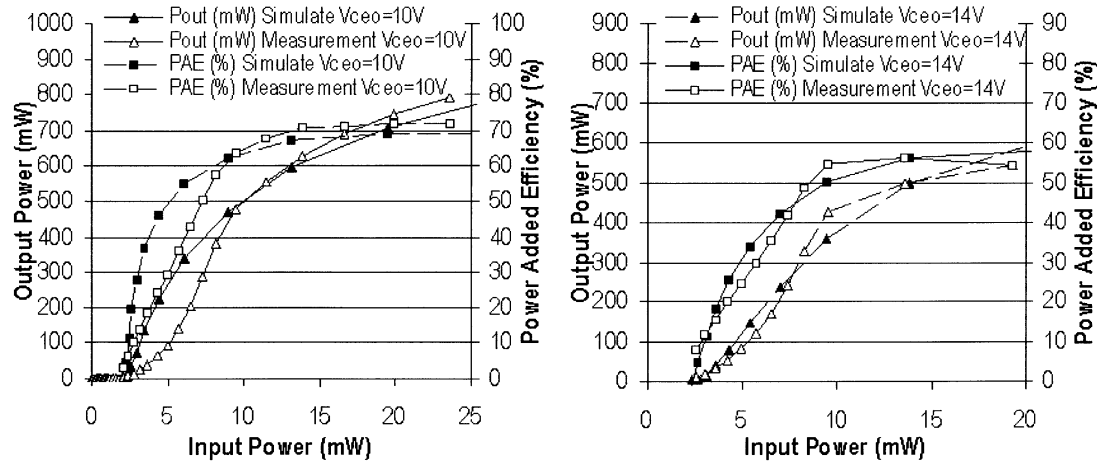


Fig. 9. Output power and power added efficiency versus input power measured and simulated on C-class ( $V_{beo} = 0$  V) at 2 GHz for various collector bias voltages (10 V, 14 V). Load was modified between each measurement for maximum output power.

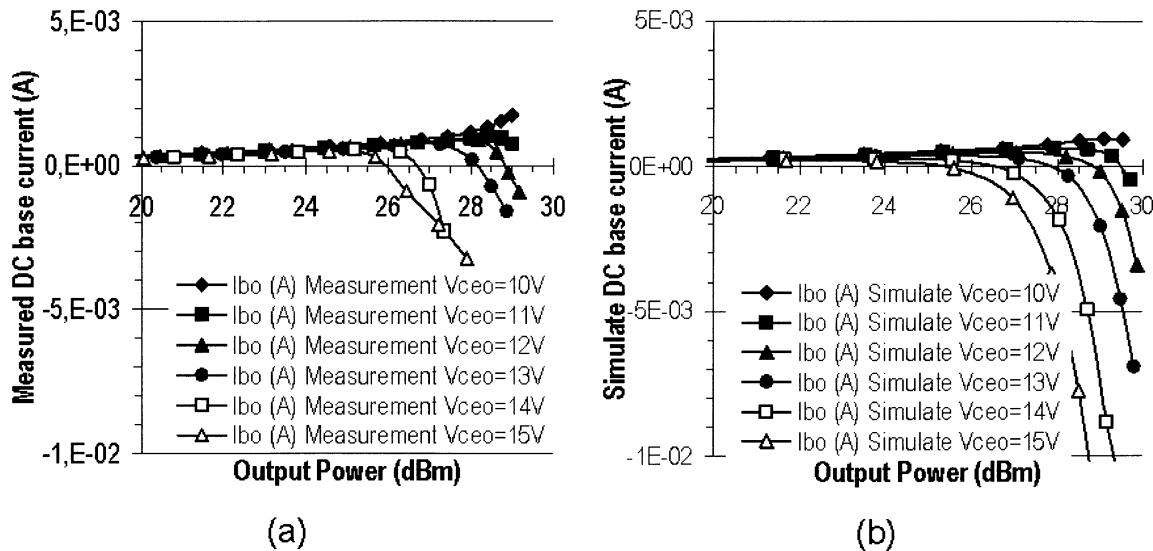


Fig. 10. Comparison between average base current versus output power measured (a) and simulated (b).

( $I_B = 0.1$   $\mu$ A). Six fingers of a  $2 \times 30$   $\text{mm}^2$  HBT coming from the HB20P process developed by UMS was used for the measurements. During the large-signal measurements, the transistor was biased with a constant dc base-emitter voltage  $V_{BE} = 0$  V, corresponding to a class C operation mode.

The input/output power characteristics and the dc base and collector currents were recorded for different values of the collector emitter bias voltage (from  $V_{CE} = 10$  V until 15 V). For each value, the load impedance was tuned looking for a maximum output power. At high output power, the maximum collector current was limited regarding its maximum value define by the Kirk effect.

Fig. 9 shows power measurements and Fig. 10 gives a comparison between measurements and simulations. The model presented in this paper claims its ability to fit the breakdown behavior of HBTs. The negative value of the base current shows that the RF signal goes beyond the  $BV_{CE0}$  voltage and swings in the BC avalanche area. This trend demonstrates the ability of HBTs to operate at very high collector voltage without failure as far as the base biasing is carefully controlled.

### III. ENHANCED MODELING FOR TEMPERATURE DEPENDENCE OF THERMAL RESISTANCE $R_{TH}$ AND Emitter Resistance

#### A. Continuous Wave (CW) Thermal Resistance Extraction

By using our pulsed measurement set-up, we are able to measure isothermal diode characteristics. The method used to extract thermal resistance is a coincidence method [12]. We plot on the same graph isothermal and CW  $I_B = f(V_{BE})$  curve. By this way, on the intercept point of an isothermal and a CW curve, we know both the dissipated power and the temperature which enable us to calculate the thermal resistance (Fig. 11) by the well-known equation

$$R_{TH} = \frac{T_J - T_{Case}}{\text{Dissipated.power} = V_{CE0} \cdot I_{C0} + V_{BE0} \cdot I_{B0}}. \quad (6)$$

#### B. Transient Thermal Response Modeling

The previous method allows us to know a steady-state thermal resistance, we cannot access to the transient response.

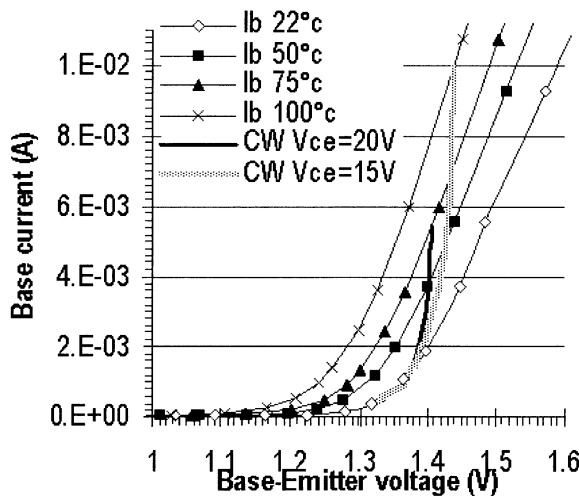


Fig. 11. Thermal resistance extraction by the interception of CW and pulse measurement.

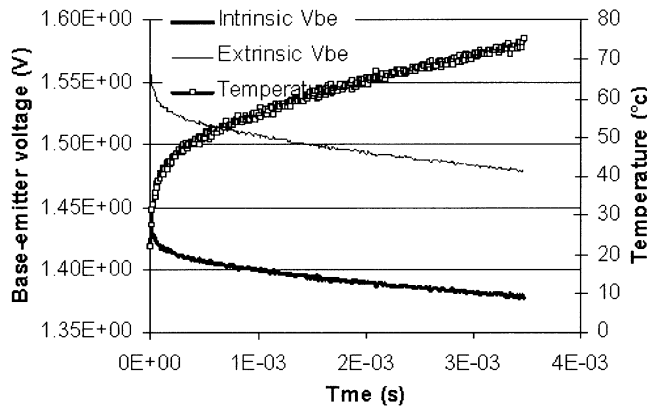


Fig. 12. Transient thermal response of 16 finger of  $2 \times 70 \mu\text{m}^2$  where initial thermal temperature is set to  $22^\circ\text{C}$ .

For that kind of response, we use a base-emitter pulse time-domain waveform in order to identify the different time constants of the thermal response. Such a response is very important for radar applications in which pulsed mode is required. We have to know the evolution of the temperature during a pulse to predict accurately the phase shift observe during the large-signal measurement [13]. With an oscilloscope, we access to the extrinsic base-emitter voltage, the intrinsic voltage is derive with the difference

$$V_{\text{BEintrinsic}} = V_{\text{BEextrinsic}} - R_E \cdot I_E \approx V_{\text{BEextrinsic}} - R_E \cdot I_C. \quad (7)$$

It is then possible to observe a transient thermal representation during a pulse (Fig. 12). It should be noted that during the measurement, the first  $10 \mu\text{s}$  could not be analyzed because of the large time analysis windows which induces an incertitude on the value of  $V_{\text{BE}}$  and operating temperature close to  $40^\circ\text{C}$  in the beginning of the measurement.

Three-dimensional (3-D)-thermal simulations are used to complete the modeling and extract a complete thermal circuit make of  $N$  time  $RC$  networks. The topology of the thermal network is depicted on Fig. 13 and should replace the single  $RC$  network on Fig. 4. Parameters used on that network are

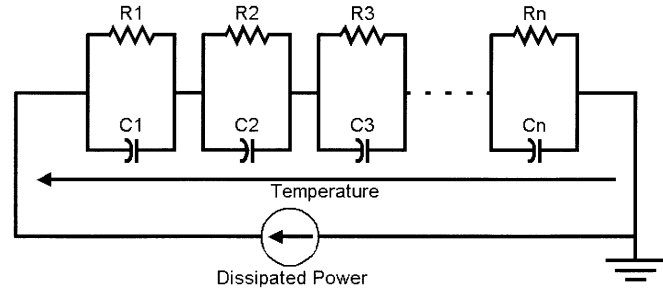


Fig. 13. Thermal network.

the following:  $N$  the number of  $RC$  cells, thermal resistances  $R_i$  and time constants  $\tau_i$  where thermal capacitances  $C_i$  are defined as follows:

$$\tau_i = R_i \cdot C_i \quad (8)$$

and where

$$\sum_{i=1}^N R_i = R_{\text{THSteady.state}} \quad (9)$$

where the  $R_{\text{THSteady-state}}$  value is obtained by the coincidence method.

This is a global thermal modeling for multi-finger devices. It exhibits a short computation time on commercial CAD software because of its simpler implementation (only  $RC$  network) compared to a distributed finger approach that is more accurate but needs more computation time. That kind of model has been developed and explained in [14].

Using five  $RC$  networks gives excellent results on the temperature evolution as it can be seen in Fig. 14. Constant times vary from  $3.10^{-8}$  to  $1.10^{-2}$  s. In Fig. 15, we plot on the same graph the measurements and the model of the thermal transient response.

### C. Thermal Effects on Emitter Resistance

Static nonlinear parameters extraction has shown the effects of operating temperature on the value of the emitter resistance. As a matter of fact, a decrease of its value is observed with an increase of the operating temperature. It affect the static characteristics of the device ( $V_{\text{BE}} = f(V_{\text{CE}})$  curve and the RF characteristics [maximum stable gain (MSG)]. The emitter resistance has a predominant effect on gain value. A linear variation law of  $R_E$  with temperature has been defined as shown in the model

$$R_E = -0.0023 \cdot T + 1.45 \quad (10)$$

where  $T$  is the operating temperature in kelvin.

In Fig. 16(a), we present the small-signal power gain measured at different operating temperatures on quasi-isothermal conditions where the effects previously described are present. In Fig. 16(b) (simulations with constant  $R_E$ ) no significant modification of the MSG can be observed, and the tendencies are in contradiction with measurements. Finally, in Fig. 16(c), a temperature dependent emitter resistance was included during simulations and enables us to observe the same tendencies than the measured MSG.

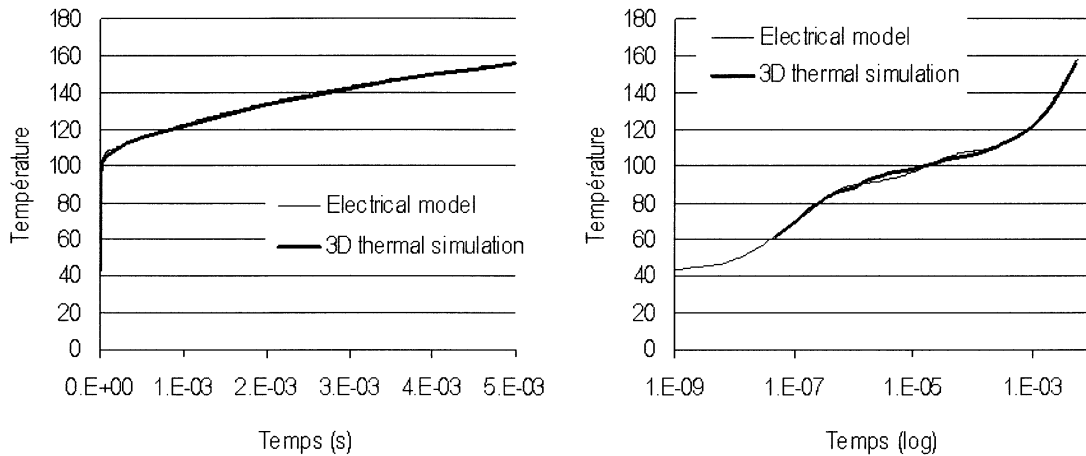


Fig. 14. Comparison between thermal circuit response (thin curve) and 3-D thermal simulation (thick curve).

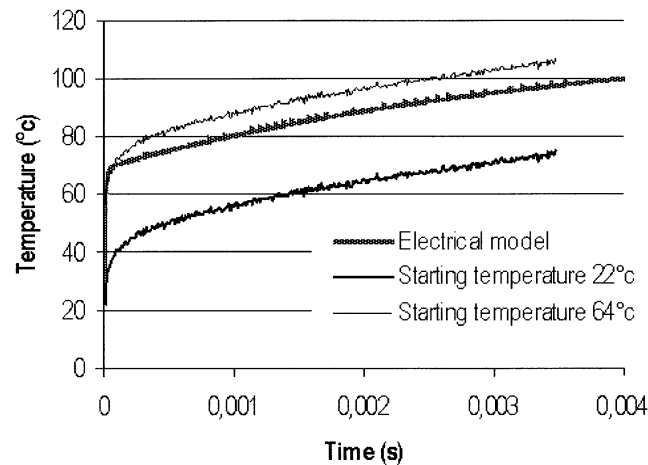


Fig. 15. Comparison between electrothermal model and measurement with two initial temperature to take into account the incertitude on the first 10  $\mu$ s.

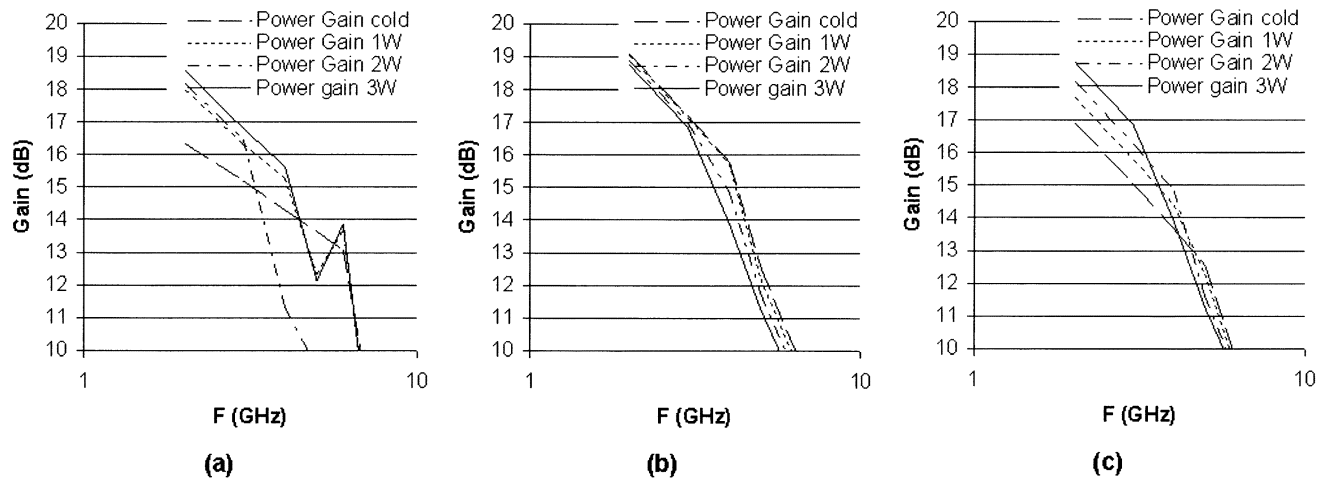


Fig. 16. Maximum power gain and MSG for different operating temperature defined by a dissipated power in three cases on a 20 finger of  $3 \times 70 \mu\text{m}^2$ . (a) Measurements. (b) Simulation with constant emitter resistance. (c) Simulation with temperature dependent emitter resistance.

Such a variation leads to an increase of small-signal power gain with operating temperature but is not in agreement with the ballast role of this resistance more effective at high temperature.

It can be observe on Fig. 16(a) and (c) some discrepancies at low dissipated power between measurement and modeling

with thermal dependent emitter resistance on the MSG. However, modeling is more accurate at high dissipated power. It must be noted that this small-signal gain have been obtain from the full nonlinear electrothermal model which does not take into account nonlinear thermal resistance.

#### IV. CONCLUSION

A lot of experiences confirm the ability of the HBTs to operate above the  $BV_{ceopen}$  breakdown voltage. The influence of such operating mode is established and a new nonlinear HBT model taking into account this effect is proposed. Physical simulations were performed to investigate the effect of breakdown on a macroscopic scale in order to justify our model choice. It has been proved that the dc current variations are useful to detect if the transistor work in the breakdown area during load-pull measurement. Negative base current over 10 mA was achieved without any damage of the device.

Measurements and modeling of the HBT under high RF swings show good agreement thus assessing the model accuracy. Furthermore, an advanced electrothermal network has been presented to replace and complete existing solution that is too much inaccurate for pulse operating mode where the thermal state has dynamic effect. The thermal network has been obtained by isothermal dc measurements, long pulse time domain base-emitter voltage waveform measurements and 3-D thermal simulations.

#### ACKNOWLEDGMENT

The authors would like to thank United Monolithic Semiconductors (UMS), Orsay Cedex, France, for supporting this work.

#### REFERENCES

- [1] I. Takenaka, K. Ishikura, K. Takahashi, K. Kishi, Y. Ogasawara, K. Hasegawa, H. Takahashi, F. Emori, and N. Iwata, "A 240 W power heterojunction FET with high efficiency for W-CDMA base stations," in *IEEE MTT-S Int. Microwave Symp. Dig.*, 2001, pp. 645-648.
- [2] D. Floriot *et al.*, "Power HBT technologies: Present and trends," in *GaAs Symp. Dig.*, Sept. 2001, pp. 57-60.
- [3] P. Kurpas *et al.*, "High-voltage GaAs power-HBT's for base-station," in *IEEE MTT-S Int. Microwave Symp. Dig.*, 2001, pp. 633-636.
- [4] R. Anholt, "Physical compact collector-emitter breakdown model for heterojunction bipolar transistors," *Solid-State Electron.*, vol. 41, no. 11, pp. 1735-1737, 1997.
- [5] H. C. Poon and J. C. Meckwood, "Modeling of Avalanche effect in integral charge control model," *IEEE Trans. Electron Devices*, vol. ED-19, Jan. 1972.
- [6] W. J. Kloosterman and H. C. de Graaff, "Avalanche multiplication in a compact bipolar transistor model for circuit simulation," *IEEE Trans. Electron Devices*, vol. 36, pp. 1376-1380, July 1989.
- [7] R. Sommet, Y. Perréal, and R. Quéré, "A direct coupling between the semiconductor equation describing a GaInP/GaAs HBT in a circuit simulator for the co-design of microwave devices and circuits," in *GaAs Symp. Dig.*, Sept. 1997, pp. 149-152.
- [8] G. Gao, H. Morkoç, and M. C. F. Chang, "Heterojunction bipolar transistor design for power application," *IEEE Trans. Electron Devices*, vol. 39, pp. 1987-1997, Sept. 1992.
- [9] J. P. Fraysse *et al.*, "A non quasi static model of GaInP/GaAs HBT for power applications," in *IEEE MTT-S Int. Microwave Symp. Dig.*, vol. 1, 1997, pp. 379-382.
- [10] C.-J. Wei, J. C. M. Hwang, W.-J. Ho, and J. A. Higgins, "Large signal modeling of self-heating, collector transit time, and RF-breakdown effects in power HBT's," *IEEE Trans. Microwave Theory Tech.*, vol. 44, pp. 2641-2647, Dec. 1996.
- [11] J.-P. Teyssié *et al.*, "40-GHz/150-ns versatile pulsed measurement system for microwave transistor isothermal characterization," *IEEE Trans. Microwave Theory Tech.*, vol. 46, pp. 2043-2052, Dec. 1998.
- [12] T. Peyretaille *et al.*, "A pulsed-measurement electrothermal model for HBT with thermal stability prediction capabilities," in *IEEE MTT-S Int. Microwave Symp. Dig.*, June 1997, pp. 1515-1518.

- [13] C. Arnaud *et al.*, "An active pulsed RF and pulse DC load-pull system for the characterization of power transistors used in coherent radar and communication system," in *IEEE MTT-S Int. Microwave Symp. Dig.*, 2001, pp. 1463-1466.
- [14] D. Lopez, R. Sommet, and R. Quéré, "Spice thermal subcircuit of multi-finger HBT derived from Ritz vector reduction technique of 3D thermal simulation for electrothermal modeling," in *GaAs Symp. Dig.*, 2001, pp. 207-210.



**Sylvain Heckmann** was born in Beaune, France, on December 21, 1977. He received the postgraduate diploma in microwave communications from the University of Limoges, Limoges, France, in 2000, and is currently working toward the doctor degree in electronic engineering with the Microwave Laboratory, University of Limoges.

His research area of interests are HBT power amplifier design and nonlinear device modeling.



**Raphaël Sommet** was born in Firminy, France, in 1967. He received the Ph.D. degree in electrical engineering from the University of Limoges, Limoges, France, in 1996.

He is currently a permanent Researcher of the French National Research Center (CNRS) and works with the Institut de Recherche en Communications Optiques et Microondes (IRCOM) Laboratory, University of Limoges. His research interests concern device physical modeling especially for HBTs, 3-D thermal modeling, and model reduction techniques,

and generally CAD techniques for coupling physical approach for device and circuit simulation.



**Jean-Michel Nébus** was born in Bourganeuf, France, on April 13, 1963. He received the Ph.D. degree in communication engineering from the University of Limoges, Limoges, France, in 1988.

From 1988 to 1990, he was an Engineer with ALCATEL ESPACE, Toulouse, France, where he was involved with the TELECOM 2 Satellite payload development. In 1990, he rejoined the University of Limoges, as a Teacher and Researcher in microwave circuits.

**Jean-Claude Jacquet**, photograph and biography not available at time of publication.



**Didier Floriot** received the Electrical Engineering degree from the Ecole Supérieure d'Electricité (ESE), France, in 1992, and the Ph.D. degree from the University of Paris VI, Paris, France, in 1995. His doctoral research was focused on the development of high-power InGaP HBT technology.

He is currently a Group Manager with the Thales Research and Technology Laboratory, Orsay, France, where he is currently involved in the development of high power microwave devices (III-V HBT wide-bandgap semiconductors) and cooling techniques



**Philippe Auxemery** was born in Limoges, France, in 1963. He received the Ph.D. degree in electronics from the University of Limoges, Limoges, France, in 1989.

In 1989, he joined the GaAs Monolithic Microwave Circuit Department, Thomson-CSF, where he was involved with the modeling of power MESFETs for monolithic microwave integrated circuits (MMICs). Since 1996, he has been with United Monolithic Semiconductors (UMS), Orsay Cedex, France, where he is involved with the development and modeling of HBTs for MMICs.



**Raymond Quéré** (M'88–SM'99) received the Engineer and French Aggregation degrees in applied physics from ENSEEIHT Toulouse, Toulouse, France, in 1976 and 1978, respectively, and the Ph.D. degree from the University of Limoges, Limoges, France, in 1989.

In 1989, he was appointed Professor with the Technology Institute of Electrical Engineering (IUT), Brive, France, where he is involved in research dealing with nonlinear design and modeling of microwave circuits, with a special emphasis on

nonlinear stability analysis of potentially unstable circuits such as oscillators, frequency dividers, and power amplifiers. He is also strongly involved with nonlinear characterization and modeling of microwave active devices based on pulsed measurements techniques.

Dr. Quéré is a member of the Technical Committee of the European Microwave Conference (EuMC). He has served as a reviewer for the IEEE TRANSACTIONS ON MICROWAVE THEORY AND TECHNIQUES.